ly apparent why the Rees iterations yield the exact time evolution in the limit of an infinitely large self-scattering rate. It is also demonstrated that the notion of self-scattering can be generalized to allow for negative self-scattering rates, in direct violation of a condition imposed by Rees. It is even shown for one model that for certain choices of the model parameters, the optimum self-scattering rate may be negative everywhere.

The models are also used to discuss various methods of evaluating the first-order corrections to the steady state resulting from a small perturbation in the system. It is shown that the summations arising must be treated carefully, and consistently, lest the results obtained be simply incorrect.

The advantages of the models for the evaluation of numerical and analytic approximation procedures used in calculating other hot-electron properties, for which the models will usually yield exact solutions, need hardly be stressed.

---

[1]P. C. Kwok and T. D. Schultz, preceding paper, Phys. Rev. B 3, 1180 (1971), hereafter called I.
[2]H. D. Rees, J. Phys. Chem. Solids 30, 643 (1969).
[3]P. J. Price, IBM J. Res. Develop. 14, 12 (1970).
[4]H. F. Budd, Phys. Rev. 158, 798 (1967).
[5]H. D. Rees, J. Phys. C 3, 965 (1970).
[6]In some ways this is a model for any physical situation where there are two valleys in $\vec{k}$ space, sufficiently removed from one another that one can neglect the orbits that link them. There is, unfortunately, one important respect in which the interesting physical situations differ from the models. In the physical situations, the *intervalley* scattering rate varies dramatically with position within the initial valley.

PHYSICAL REVIEW B VOLUME 3, NUMBER 4 15 FEBRUARY 1971

Thermal and Electrical Transport in a Tungsten Crystal for Strong Magnetic Fields and Low Temperatures*

Jerome R. Long
Department of Physics, Virginia Polytechnic Institute and State University, Blacksburg, Virginia 24061
(Received 1 July 1970)

Direct-current electrical and thermal transport coefficients were experimentally determined in a very pure tungsten crystal at six temperatures in the range 1.4–4.1 K and at magnetic fields up to 22 kOe. The field was applied along a [100] axis and each of the coefficients measured along an equivalent ⟨100⟩ direction. Kinetic coefficients computed from the data were interpreted in terms of a Sondheimer-Wilson–type multiband relaxation-time model. The results were generally consistent with the extensive literature on the fermiology of tungsten. Galvanomagnetic data were approximately independent of temperature, a result implying elastic scattering and a common relaxation time for all transport effects, but the field dependence and magnitude of the thermal and Righi-Leduc resistivities were both distinctly less than those predicted by the Wiedemann-Franz law when a reasonable value of the lattice conductivity was assumed. A density of states computed from the Nernst-Ettingshausen coefficient was consistent with values reported from specific-heat measurements, but displayed an anomalous temperature dependence similar to that of the Righi-Leduc coefficient.

I. INTRODUCTION

The temperature and magnetic field dependence of six galvanomagnetic and thermomagnetic transport coefficients of a tungsten monocrystal are reported here. The dc measurements were performed at liquid-helium-4 temperatures in magnetic fields up to 22 kOe directed along a [100] axis transverse to the plane of the effects in the body-centered-cubic (bcc) crystal.

Provided the magnetic field is applied along an axis of three-, four-, or sixfold rotational symmetry, and the electrical and thermal fluxes are constrained to the plane normal to that axis, only six kinetic transport coefficients are required to determine all of the thermogalvanomagnetic phenomena in a metallic crystal. The transverse-even effects vanish, and the six kinetic coefficients are calculable in terms of only six measurable nonkinetic coefficients. This is a consequence of the Onsager relations.[1,2]

A study of transport phenomena is motivated by two distinct, but coupled, goals. First, one would like to use the transport effects as a tool for investigating the structure and dynamics of the electron–lattice-defect system in a class of materials. Second, one wishes to understand mechanisms present in the transport process and to determine

the relative importance of those mechanisms which are active in a given material under a specific set of conditions. The measurements reported here were primarily directed toward the second of these goals. The successes of Fermi-surface studies[3] over the past decade have made it possible to seek a much more detailed interpretation of transport processes on the Fermi surface than was possible earlier. Improvements in experimental facilities and sample quality are also very significant.

Many of the extant transport data were obtained when our knowledge of Fermi surfaces was poor. In addition, the large impurity content of most samples resulted in a masking of the intrinsic scattering mechanisms at low temperatures, a situation which may actually favor the first of the above-stated goals, but which severely limits the second. Tungsten is representative of the above situation.

Tungsten, a transition metal of the sixth group and period, has been available in monocrystalline form with relatively high purity for a longer time than most other metals. The behavior of electrical and thermal transport coefficients of tungsten in a magnetic field was investigated as early as 1936 by Justi and Scheffers[4] and by Grüneisen and Adenstedt.[5] An extended series of measurements of the thermal and electrical magnetoresistivities by de Haas and de Nobel[6] and de Nobel[7,8] are particularly relevant to the thermal measurements reported here. Except for the relatively high-temperature work of van Witzenburg and Laubitz,[9] work on the very-high-purity tungsten now available has not considered the problem of thermal transport. The electrical resistivity has been studied by Berthel[10] and by Volkenshteyn *et al.*,[11] while the galvanomagnetic effects were measured by Fawcett,[12] by Fawcett and Reed,[13] and by Volkenshteyn *et al.*[14] The low-temperature magnetothermoelectric, Nernst, and Righi-Leduc effects reported here do not appear to have been studied previously.

References to the extensive experimental literature on the closed compensated Fermi surface of tungsten may be found in the de Haas–van Alphen work of Girvan, Gold, and Phillips,[15] while theoretical APW (augmented-plane-wave) band-structure calculations were done by Loucks[16] and by Mattheiss[17] following the model of Lomer.[18]

In Sec. II, the phenomenological definitions and elementary microscopic theory of the magnetotransport coefficients are reviewed. Section III deals with pertinent experimental aspects of the work. The results and an elementary interpretation of each type of measurement are then presented. A more detailed interpretation of certain parts of this work will be found in a following paper. All of the measurements reported pertain to transport effects with a monotonic dependence on the magnetic field. Oscillatory phenomena due to size effect[19] or Landau quantization[20] were not measured.

II. THEORY

The Onsager formulation[1,2] of the thermodynamics of irreversible processes has resulted in a rigorous phenomenological framework for defining the magnetotransport coefficients. The kinetic coefficients of the thermogalvanomagnetic effects are tensors defined by the kinetic equations[21]

$$\begin{aligned}\vec{J} &= \vec{\vec{\sigma}}\vec{E} + \vec{\vec{\epsilon}}''\vec{\nabla}T,\\ \vec{U} &= -\vec{\vec{\pi}}''\vec{E} - \vec{\vec{\lambda}}''\vec{\nabla}T,\end{aligned} \tag{1}$$

which express the fluxes $\vec{J}$, the electric-current density, and $\vec{U}$, the heat-current density, as linear combinations of the affinities $\vec{E}$, the effective emf (which includes the thermodynamic force associated with the chemical potential of the electronic carriers and plays the role of the measurable electric field), and the temperature gradient $\vec{\nabla}T$. The kinetic coefficients so defined are: $\vec{\vec{\sigma}}$, the electrical conductivity; $\vec{\vec{\lambda}}''$, the thermal conductivity; $\vec{\vec{\epsilon}}''$, the thermoelectric tensor; and $\vec{\vec{\pi}}''$, the Peltier tensor. Only one of the tensors $\vec{\vec{\epsilon}}''$ and $\vec{\vec{\pi}}''$ is independent, since by the Onsager-Kelvin relation $\vec{\vec{\pi}}'' = T\vec{\vec{\epsilon}}''$. For effects measured in the [100] plane normal to the magnetic field, the independent tensors $\vec{\vec{\sigma}}$, $\vec{\vec{\lambda}}''$, and $\vec{\vec{\epsilon}}''$ each reduce to a 2×2 form with two independent elements in each tensor. The total number of independent coefficients is thus six. The $\vec{\vec{\sigma}}$ tensor is, for instance,

$$\vec{\vec{\sigma}} = \begin{pmatrix}\sigma_{xx} & \sigma_{xy}\\ \sigma_{yx} & \sigma_{yy}\end{pmatrix} = \begin{pmatrix}\sigma_{11} & \sigma_{12}\\ -\sigma_{12} & \sigma_{11}\end{pmatrix}$$

if the magnetic field is applied along a threefold or higher $z \to 3$ direction and the affinities and fluxes are measured in orthogonal $x \to 1$ and $y \to 2$ directions.

The phenomenological *kinetic* coefficients are most important because kinetic coefficients relate directly to the results of microscopic theory where it is customary to calculate $\vec{J}$ and $\vec{U}$. The conventional microscopic theory of transport phenomena assumes validity of a Boltzmann transport equation and the fundamental problem is then to solve the equation for the distribution function $f_{\vec{k}}$ for specific conditions of symmetry, thermodynamic affinities, and other parameters. One then calculates

$$\vec{J} = \frac{e}{4\pi^3}\int \vec{v}_{\vec{k}} f_{\vec{k}}\, d\vec{k}, \qquad \vec{U} = \frac{1}{4\pi^3}\int \vec{v}_{\vec{k}} (\mathcal{E}_{\vec{k}} - \zeta) f_{\vec{k}}\, d\vec{k}, \tag{2}$$

where $\vec{v}_{\vec{k}}$ is the velocity of an electronic carrier of charge e, energy $\mathcal{E}_{\vec{k}}$, chemical potential ζ, and wave vector $\vec{k}$. A calculation of the currents by (2) leads to expressions in which the kinetic coefficients defined by (1) may be identified as the

coefficients of $\vec{E}$ and $\vec{\nabla}T$.

A tractable comparison of all six experimentally determined kinetic coefficients with microscopic theory is possible at present only for rather simplified models. The most useful of these has been the Sondheimer-Wilson[22] model, which assumes conduction by independent quadratic bands of carriers of either sign, each achieving equilibrium by a relaxation process and each contributing additively to the total current. The Sondheimer-Wilson (SW) results[23] as modified by Grenier[24,25] are summarized in Gaussian units as follows:

magnetoconductivity,

$$\sigma_{11} = ec\sum_i \frac{n_i a_i H_i}{H^2 + H_i^2}; \tag{3a}$$

Hall conductivity,

$$\sigma_{12} = ec\sum_i (\pm)\frac{n_i H}{H^2 + H_i^2}; \tag{3b}$$

magnetothermopower,

$$\epsilon''_{11} = \frac{\pi^2 k_B^2 cT}{3}\sum_i (\pm)\frac{Z_i a_i H_i}{H^2 + H_i^2}; \tag{3c}$$

Nernst or Nernst-Ettingshausen coefficient,

$$\epsilon''_{12} = \frac{\pi^2 k_B^2 cT}{3}\sum_i \frac{Z_i H}{H^2 + H_i^2}; \tag{3d}$$

thermal magnetoconductivity,

$$\lambda''_{11} = \lambda''_g + \lambda''_{e11} = \lambda''_g + L_1 T\sigma_{11}; \tag{3e}$$

Righi-Leduc conductivity,

$$\lambda''_{12} = L_2 T\sigma_{12}. \tag{3f}$$

In these expressions H is the magnetic field applied normal to $\vec{J}$ and $\vec{U}$, and T is the Kelvin temperature. The symbols π, e, c, and k_B are constants having their conventional meaning. The other symbols represent properties of the crystal. The ith band contains n_i carriers, which, if hole- (electron-) like, takes the + (−) sign as indicated in Eqs. (3b) and (3c). The mobility μ_i of the carriers is represented by the relaxation field $H_i = c/\mu_i = m_i^* c/e\tau_i$, where τ_i is the relaxation time and m_i^* is the cyclotron effective mass. For a band of cyclotron frequency ω_{ci}, H_i is the applied field for which $\omega_{ci}\tau_i = 1$. The magnitudes of the thermoelectric coefficients are determined by Z_i, the density of states of the ith band. The quantity a_i is a mass anisotropy factor which takes the value unity for a spherical Fermi surface.[24,25] The thermal conductivities are given in terms of the electrical conductivities, where L_j is the Lorenz number. Strict validity of these SW expressions is limited to elastic scattering, in which case $L_j = L_0 = \pi^2 k_B^2/3e^2 = 2.445\times 10^{-8}\ \mathrm{V^2 K^{-2}}$. The electronic component λ''_{e11} of the thermal conductivity is supplemented by λ''_g, the lattice thermal conductivity,[26] which will be considered separately, from the SW theory of the electronic effects.

The physical conditions which lead to Eqs. (1)–(3) imply control of $\vec{E}$ and $\vec{\nabla}T$ as independent variables, a condition not readily attained in the laboratory. The practical experimental arrangements are the following: (a) One immerses the sample in an isothermal bath and controls $\vec{J}$ and $\vec{\nabla}T$, in which case a set of isothermal coefficients is defined by the equations

$$\begin{aligned}\vec{E} &= \overleftrightarrow{\rho}\,\vec{J} - \overleftrightarrow{\epsilon}\,\vec{\nabla}T,\\ \vec{U} &= -\overleftrightarrow{\pi}\,\vec{J} - \overleftrightarrow{\lambda}\,\vec{\nabla}T;\end{aligned} \tag{4a}$$

or (b) one connects one end of the sample to a thermal reservoir, while thermally isolating the bulk of the sample in a high vacuum. These transverse adiabatic conditions imply control of $\vec{J}$ and $\vec{U}$, in which case a set of "adiabatic" coefficients is defined by the equations

$$\begin{aligned}\vec{E} &= \overleftrightarrow{\rho}'\vec{J} + \overleftrightarrow{\epsilon}'\vec{U},\\ \vec{\nabla}T &= -\overleftrightarrow{\pi}'\vec{J} - \overleftrightarrow{\gamma}\,\vec{U}.\end{aligned} \tag{4b}$$

In this work, both sets of experimental conditions were utilized in order to measure two elements each of the isothermal resistivity tensor $\overleftrightarrow{\rho}$, the "adiabatic" thermal resistivity tensor $\overleftrightarrow{\gamma}$, and the "adiabatic" thermoelectric tensor $\overleftrightarrow{\epsilon}'$.

Microscopic theory calculates kinetic coefficients, but an experiment does not measure them. A popular practice found in the literature of transport phenomena is to "invert" the expressions obtained from a microscopic theory into the form of the experimental coefficients. In the present work, the experimental coefficients have, instead, been inverted into kinetic form. Presentation of the measurements in kinetic form offers several advantages. Any simplifying approximations made in the inversions are determined by the experimentally observed magnitudes of the coefficients and do not involve additional assumptions in the microscopic theory. Experimental results presented in kinetic form should be more directly comparable to any new theoretical results. Finally, the physical interpretation of kinetic coefficients is usually more direct.

In general, the kinetic coefficients are obtained from the isothermal and "adiabatic" coefficients by means of Heurlinger[27] relations of the form $\overleftrightarrow{\sigma} = \overleftrightarrow{\rho}^{-1}$, $\overleftrightarrow{\lambda}'' = \overleftrightarrow{\gamma}^{-1}(\overleftrightarrow{1} + \overleftrightarrow{\epsilon}'^2\overleftrightarrow{\rho}^{-1}\overleftrightarrow{\gamma}^{-1}T)$, and $\overleftrightarrow{\epsilon}'' = \overleftrightarrow{\rho}^{-1}\overleftrightarrow{\epsilon}'\overleftrightarrow{\gamma}^{-1}$. For electronically compensated metals, it is usually possible to demonstrate, as in the present case, that some of these relations may be greatly simplified without significant error. One finds it particularly helpful that, when $H \gg H_i$, then $\overleftrightarrow{\lambda}'' \approx \overleftrightarrow{\gamma}^{-1} = \overleftrightarrow{\lambda}$ and $\epsilon''_{12} \approx \epsilon'_{12}/\rho_{11}\gamma_{11}$.

III. EXPERIMENTAL

The tungsten monocrystal was spark planed into a rectangular parallelepiped with sides nominally 19 mm long by 4 mm wide by 2 mm thick oriented normal to the ⟨100⟩ directions. It was purchased from Aremco Products, Inc. The residual resistivity ratio was found to be $\rho_{300\,K}/\rho_{1.3\,K} \approx 3\times10^4$.

All of the electrical and thermal measurements were performed using the four-terminal dc methods of Grenier *et al.*[24,25,28] The magnetic field was generated by a Ventron-Harvey-Wells L128A-FFC4 system and the dc potentials were detected with a Keithley 147 in conjunction with a Honeywell 2768 potentiometer. The sensors used in the bridge measurement of temperature differentials were Allen-Bradley $\frac{1}{10}$-W 33-Ω carbon resistors calibrated by He^4 vapor-pressure thermometry. The 67-Ω heater wound on a copper bobbin attached to the lower end of the crystal was made of W. B. Driver Cupron, as were the leads connected to the crystal, thermometers, and heater.[29]

In the thermomagnetic measurements, heat-current densities from 0.44 mW/cm^2, at the lowest temperature, to 4.6 mW/cm^2, at the highest temperature, were used in order to adjust the maximum longitudinal temperature differential to about 0.1 K. A complete set of measurements was performed at the temperatures 4.1, 3.8, 3.4, 2.6, 1.9, and 1.38 K. An electric-current density of 7.1 A/cm^2 was used.

The most persistent source of error in the absolute determination of transport coefficients is the measurement of the effective spacing of the electrical and thermal probes to the sample. Some difficulty was encountered in obtaining contacts to tungsten suitable for both electrical and thermal currents under cryogenic high-vacuum conditions. The contacts used were made by Bi-Cd soldering to a lug consisting of a 0.5-mm-wide × 5-mm-long strip of 0.003-in. gold foil which was attached to the crystal with a dot of Dupont #4922 silver preparation. The main virtue of this type of contact is that it may be completely removed by aqua regia, and leaves the crystal in pristine condition for any other measurement. The properties of these contacts were generally satisfactory except that they did not provide an ideal point contact. The probe separations of 8.34 mm for the longitudinal set and 3.86 mm for the transverse set were thus systematically uncertain by about ± 3%. Analysis of the effect of all combined systematic errors on the calculated kinetic coefficients led to a confidence of about ± 4% in the *absolute* values of the coefficients σ_{11}, λ_{11}'', and ϵ_{12}''. The coefficients σ_{12} and λ_{12}'' are only reliable to ± 8%, while the absolute precision of ϵ_{11}'' may be as poor as ± 15%. Errors in field and temperature dependences, relative values, and ratios are much less, the precision in this case being about ± 1%.

The magnetic field was oriented with respect to the crystal *in situ* for the experiment by finding the [100] minimum[12] in the electrical magnetoresistance. In that position the transverse-even voltage was null.

IV. RESULTS AND DISCUSSION

A. Galvanomagnetic (Magnetoelectric) Tensors $\overleftrightarrow{\rho}$ and $\overleftrightarrow{\sigma}$

1. *Zero-Field Measurements*

The temperature dependence (or lack) of $\rho_{11}(0, T)$, the electrical resistivity in zero applied magnetic field, is the standard indicator of the nature of the dominant scattering mechanism in a metal and, for tungsten, has been the subject of several recent studies.[10,11,30] For the crystal and conditions of this work, $\rho_{11}(0, T)$ was nearly residual, increasing by only 5% at 4.1 K over a minimum value of $(1.8 \pm 0.2)\times10^{-10}$ Ω cm at 1.3 K, which will be taken as the residual value. It is thus inferred that large-angle elastic scattering by point impurities and defects was dominant over intrinsic processes in the limitation of charge transport. Size effect was certainly also a factor.[19] A study of the intrinsic scattering and a check of Matthiessen's[31] rule from the temperature dependence of $\rho_{11}(0, T)$ was beyond the capabilities of the measuring system.

It is generally concluded[10,11,30] that the dominant low-temperature intrinsic scattering mechanism in tungsten is the electron-electron U process,[32,33] but this conclusion has been based on data taken at somewhat higher temperatures than those used here.

2. *High-Field Measurements*

In this work the term "high field" is taken to mean $H \gg H_i$ for all bands. Such is the usual condition in standard magnetoresistance studies of the Fermi-surface topology of metals[34,12] and is distinct from other uses of the term "high field" as applied to quantum-oscillatory[35] and magnetic-breakthrough[36] effects. The results of the high-field measurements of ρ_{11} and ρ_{21} are shown in Fig. 1 for the data up to H=22 kOe at 1.3 and 4.1 K.

The magnetoresistivity $\rho_{11}(H, T)$ was found to be precisely quadratic in H at all temperatures. The deviation from pure H^2 behavior for H in the ⟨100⟩ direction as reported by Fawcett[12] was not observed.

Volkenshteyn *et al.*[14] have pointed out that "the influence of temperature on the galvanomagnetic properties of metals has received very little study in the region of high fields." The temperature dependence of the ρ_{11} data reported here was small and could only be approximately determined. The criterion applied in obtaining an expression was to fit the data to the nearest integral power of T. From previous studies of $\rho_{11}(0, T)$, a T^2 relation

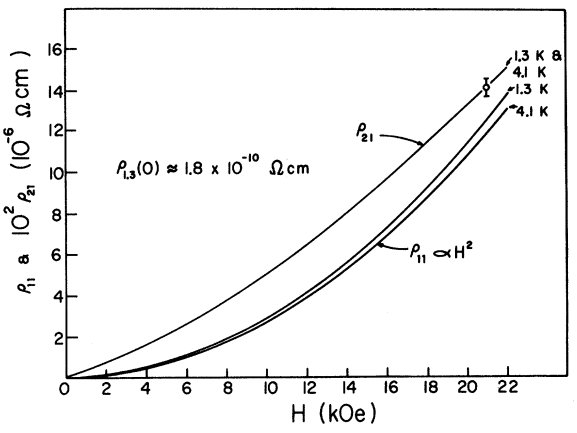

FIG. 1. Electrical resistivity tensor. Magnetoresistivity ρ_{11} and the Hall resistivity ρ_{21} are shown as functions of field and temperature. Note the temperature dependence of ρ_{11} and that ρ_{21} is roughly 1% of ρ_{11} in the upper-field range.

was expected but a T^3 relation gave a better fit to the scattered values of the small quantity $\rho_{11}(H, 0) - \rho_{11}(H, T)$. The data are approximated by either of the expressions

$$\rho_{11}(H, T) \approx \rho_{11}(0, T) + 2.86 \times 10^{-14} H^2 (1 - 7.9 \times 10^{-4} T^3), \tag{5a}$$

$$\rho_{11}(H, T) \approx \rho_{11}(0, T) + 2.87 \times 10^{-14} H^2 (1 - 3.4 \times 10^{-3} T^2). \tag{5b}$$

Although it is not well justified,[37] it is interesting to examine Eqs. (5) on the basis of a relaxation-time model. For a compensated metal in a strong field $\sigma_{11} \gg \sigma_{12}$ when the geometry is such that there is no transverse-even voltage. From Eq. (3a) one thus obtains

$$\lim_{H \gg H_i} \rho_{11}(H, T) \approx \lim_{H \gg H_i} \frac{1}{\sigma_{11}} = \frac{H^2}{c^2 \sum_i n_i a_i m_i^* / \tau_i},$$

where $\rho_{11}(0, T)$ is negligible. If Matthiessen's rule is assumed valid, then it is possible to simply add the reciprocals of the relaxation times τ_{0i} of the large-angle elastic processes (presumably due to point-defect scattering plus some size effect) contributing to the residual resistivity, and τ_{ti} of the intrinsic processes leading to a temperature-dependent resistivity. Dominance of the residual resistivity implies that $\tau_{0i}/\tau_{ti} \ll 1$. If one makes the further assumption that all of the N bands in the sum over bands are identical except for charge compensation, then

$$\lim_{H \gg H_i} \rho_{11}(H, T) \approx \left(\frac{H}{c}\right)^2 \frac{\tau_0}{Nnam^*} \left(1 - \frac{\tau_0}{\tau_t}\right).$$

Comparison of this approximation with Eqs. (5) implies either $\tau_0/\tau_t \approx 7.9 \times 10^{-4} T^3$, or $\tau_0/\tau_t \approx 3.4 \times 10^{-3} T^2$, or some intermediate relation. Application of the same arguments to $\rho_{11}(0, T)$ implies that

$$\rho_{11}(0, T) = \lim_{H \ll H_i} \rho_{11}(H, T) \approx \frac{m^*}{e^2 N n a \tau_0} \left(1 + \frac{\tau_0}{\tau_t}\right)$$

which, with the previous result, would indicate that

$$\rho_{11}(0, T) \approx \rho_{11}(0, 0) + 1.4 \times 10^{-13} T^3\ \Omega\,\text{cm}$$

or

$$\rho_{11}(0, T) \approx \rho_{11}(0, 0) + 6.1 \times 10^{-13} T^2\ \Omega\,\text{cm},$$

where $\rho_{11}(0, 0) = 1.8 \times 10^{-10}\ \Omega$cm.

The foregoing analysis is clearly too simple, and should be regarded, primarily, as a vehicle for presenting the experimental observations. It is curious, however, that little support can be found in this work for the dominance of electron-electron scattering as concluded from the T^2 law found by others.[10,11,30] The coefficient of T^2 found here is, roughly, a factor of 45 smaller than the coefficient indicated by the work of Volkenshteyn *et al.*[11] and the approximate fit [Eq. (5b)] of the data to a T^2 relation is inferior to the fit [Eq. (5a)] to a T^3 relation. A T^3 law is indicative of phonon-electron s-d scattering also commonly found in many transition metals.[30,38]

The Hall resistivity ρ_{21} (Fig. 1) exhibited a somewhat complicated field dependence and, within the precision of the measurements, was independent of temperature with a magnitude approximately 1% that of ρ_{11}. The observed behavior of ρ_{21} is readily understood by again applying the conditions $\sigma_{11} \gg \sigma_{12}$ and $H \gg H_i$ to the inversion of Eqs. (3a) and (3b). Then,

$$\lim_{H \gg H_i} \rho_{21} = \lim_{H \gg H_i} \frac{\sigma_{12}}{\sigma_{11}^2} = \frac{H^3 \sum_i (\pm) n_i - H \sum_i (\pm) n_i H_i^2}{ec(\sum_i n_i a_i H_i)^2}.$$

On the basis of this model, any observable temperature dependence of ρ_{21} must come from the temperature dependence of the relaxation time contained within the quantities H_i of each band. Therefore, if the metal is perfectly compensated [$\sum_i (\pm) n_i = 0$, but $\sum_i (\pm) n_i H_i^2 \neq 0$ except when all H_i are equal], it is only necessary that the relaxation time of each band have the same functional temperature dependence in order that ρ_{21} be independent of temperature. In the present case, compensation was complete to the extent that the term linear in H was roughly nine times as great as the cubic term at a field of 10 kOe. The very weak temperature dependence of ρ_{21} is thus quite reasonable. The positive sign and somewhat greater than linear field dependence of ρ_{21} implies that $\sum_i (\pm) n_i$ was positive but that $\sum_i (\pm) n_i H_i^2$ was negative. Therefore, holes were in the majority, and were also

TABLE I. Coefficients of the asymptotic conductivities. Comparison of the experimental results with the strong-field limits of Eqs. (3a) and (3b) yielded the tabulated quantities shown at three temperatures.

Quantity shown and units	Kinetic coefficient from which quantity is derived	Quantity at selected temperatures		
T(K)		4.1	2.6	1.4
$\sum_i n_i a_i H_i$ (10^{24} cm^{-3} Oe)	$\lim_{H\to\infty} H^2\sigma_{11}$	2.32	2.24	2.19
$\sum_i (\pm) n_i$ (10^{17} cm^{-3})	$\lim_{H\to\infty} H\sigma_{12}$	4.4	4.4	4.4
$\sum_i (\pm) n_i H_i^2$ (10^{26} cm^{-3} Oe^2)	$\lim_{H\to\infty} H^3\sigma_{12}$	−3.86	−3.57	−3.43

the more mobile carriers.

Results of the inversion of the measured quantities ρ_{11} and ρ_{21} into the kinetic quantities σ_{11} and σ_{12} are summarized (Table I) in terms of Eqs. (3a) and (3b). Inverse-square dependence of σ_{11} on magnetic field is expressed in terms of the quantity $\sum_i n_i a_i H_i$ derived from $H^2\sigma_{11}$ and Eq. (3a). The temperature dependence of $\sum_i n_i a_i H_i$ was covered in the discussion of ρ_{11}. The results for σ_{12} are expressed by putting Eq. (3b) in the form

$$\lim_{H \gg H_i} \sigma_{12} = ec\left(\frac{1}{H}\sum_i (\pm) n_i - \frac{1}{H^3}\sum_i (\pm) n_i H_i^2\right)$$

and tabulating the quantities $\sum_i (\pm) n_i$ and $\sum_i (\pm) n_i H_i^2$. Comparison of the quantity $\sum_i (\pm) n_i = 4.4 \times 10^{17}$ cm^{-3} with the number[15] $\sum_i (+) n_i = \sum_i (-) n_i = 7.4 \times 10^{21}$ cm^{-3} obtained from de Haas–van Alphen measurements indicates an excess of only 0.006% of holelike over electronlike carriers. This result supports the view that minute impurities are the sole cause of any deviation from perfect compensation of a metal which satisfies the Fawcett[39] criteria for compensation.

B. Magnetothermal Tensors $\overleftrightarrow{\gamma}$ and $\overleftrightarrow{\lambda}''$

The thermal magnetoresistivity γ_{11} and the Righi-Leduc resistivity γ_{21} are shown as functions of temperature and magnetic field in Fig. 2. In the event that thermal and electrical transport in the crystal were entirely limited by large-angle elastic (point-defect) scattering, which is the common assumption at helium temperatures, and in the absence of an appreciable conduction by the lattice, one would expect that the curves of Fig. 2 could be made to resemble quite closely those of Fig. 1 by simply multiplying all of the quantities of Fig. 2 by $L_0 T$. That is, $\overleftrightarrow{\rho}$ and $\overleftrightarrow{\gamma}$ might be connected by a straightforward application of the Wiedemann-Franz-Lorenz (WFL) relation. Such is not the case.

The most obvious dissimilarity between the $\overleftrightarrow{\rho}$ and $\overleftrightarrow{\gamma}$ data is the tendency of the Righi-Leduc resistivity to pass through a maximum, the maximum apparently moving to fields above the range of these measurements at the lowest temperatures. In addition, the product $T\gamma_{21}$ increases by approximately 65% as T is reduced from 4.1 to 1.4 K, while ρ_{21} is essentially independent of temperature. This temperature dependence of γ_{21} does not appear explicable in terms of any conventional model. It has been discussed in a brief communication[40] and will be discussed further in a following paper in terms of the kinetic coefficient λ_{12}''.

The peaking of γ_{21} is characteristic of a crystal in which the application of a magnetic field has reduced the conduction of heat by electronic carriers to a point comparable to that of the conduction of heat by the lattice. Larger fields must be applied to achieve this peaking at lower temperatures because the lattice conductivity is smaller at lower temperatures. A further discussion of the peaking of γ_{21} can be found in a study of antimony,[28,41] where the effect was considerably more pronounced.

The direct effect of an apparently appreciable lattice conductivity (which is itself essentially independent of the magnetic field) at the fields of these measurements was the reduction of the pure quadratic field dependence of ρ_{11} to an effective $H^{1.6}$ dependence of γ_{11} (Fig. 2). At fields of 60–80 kOe and above, the γ_{11} of this crystal should have saturated to values characteristic of the lattice conductivity and independent of H. An example of

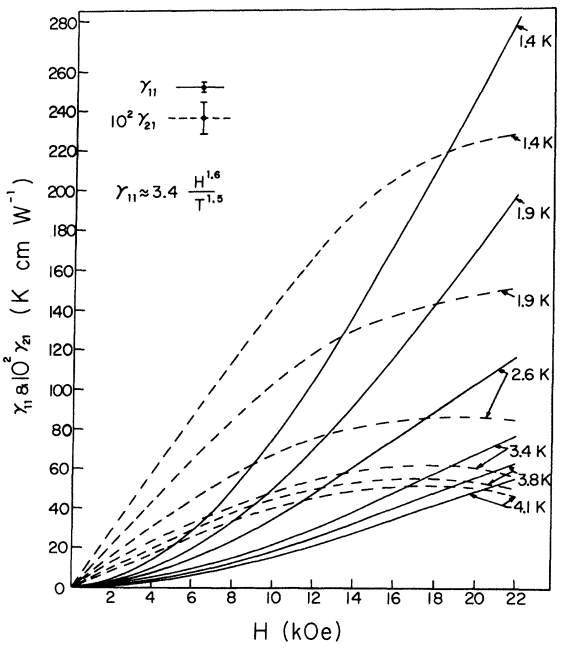

FIG. 2. Thermal resistivity tensor. Thermal magnetoresistivity γ_{11} and the Righi-Leduc resistivity γ_{21} are shown as functions of field and temperature. Note that γ_{11} is less than quadratic in H and that γ_{21} tends to pass through a maximum at a value that is roughly 1% of γ_{11}.

the complete saturation of γ_{11} due to lattice conduction was reported at much lower fields in the antimony papers[28,42] and the tendency to saturation as observed here in tungsten at liquid-helium temperatures was studied extensively for tungsten in the scattering regime of liquid-hydrogen temperatures by de Nobel.[6–8] The term "saturation" as applied here to the effect of lattice conduction on γ_{11} should not be mistaken for the ordinary saturation of both ρ_{11} and γ_{11} in uncompensated metals or saturation due to magnetic breakthrough in normally compensated metals.[34,36] Lattice conduction will be discussed further in a following paper.

It can be seen (Fig. 2) that γ_{11} depends on temperature approximately as $T^{-1.5}$ over the range of temperatures studied, rather than with the T^{-1} dependence predicted by the WFL relation. The product $T\gamma_{11}$ is considerably more dependent upon temperature than ρ_{11}. While ρ_{11} increases by about 7% as T varies from 4.1 to 1.3 K at 22 kOe, the product $T\gamma_{11}$ increases by 70% over roughly the same interval. Although lattice conduction accounts for some of this variation, it is not nearly sufficient to account for all of it.

The assumption of a single relaxation time common to both electrical and thermal processes is implicit in Eqs. (3). The excess temperature dependence of $T\gamma_{11}$ is not consistent with the assumption of a single relaxation time. The common inference, that a single relaxation time is dominant when the residual part of the zero-field resistivity $\rho_{11}(0, T)$ is dominant, appears to be valid only for electrical processes. Small-angle scattering, which has a rather minor effect upon ρ_{11}, can be very effective upon γ_{11} via the vertical process.[42]

The failure of $\vec{\vec{\gamma}}$ data to conform to a straightforward Sommerfeld version of the WFL relation does not rule out the possibility of fitting the data to more general relations of the form of Eqs. (3e) and (3f), as will be seen in a following paper. If this is to be done, the data must be converted into $\vec{\vec{\lambda}}''$ form. The conversion involves the lengthy tensor manipulation $\vec{\vec{\lambda}}'' = \vec{\vec{\gamma}}^{-1}(\hat{1} + \vec{\vec{\epsilon}}'^{2}\vec{\vec{\rho}}^{-1}\vec{\vec{\gamma}}^{-1}T)$. In general, these manipulations may seriously compound errors in the measured quantities. However, for compensated metals at high fields and low temperature, it turns out that, to a precision of 1% or better,

$$\lambda_{11}'' \approx \frac{1 - \epsilon_{21}'^{2}T/\rho_{11}\gamma_{11}}{\gamma_{11}}, \quad \lambda_{12}'' \approx \frac{\gamma_{21}(1 - 2\epsilon_{21}'^{2}T/\rho_{11}\gamma_{11})}{\gamma_{11}^{2}},$$

with the correction term $\epsilon_{21}'^{2}T/\rho_{11}\gamma_{11}$ usually being small. For the present tungsten data at 20 kOe, the correction ranges from 0.3% at 1.4 K to 1.7% at 4.1 K. The kinetic thermal conductivities λ_{11}'' and λ_{12}'' can thus be computed from the experimental data with nearly the same precision as the electrical conductivities σ_{11} and σ_{12}.

C. Magnetothermoelectric Tensors $\vec{\vec{\epsilon}}$, $\vec{\vec{\epsilon}}'$, and $\vec{\vec{\epsilon}}''$

The "adiabatic" thermoelectric tensor $\vec{\vec{\epsilon}}'$, as defined by Eqs. (4b), was measured. Raw $\vec{\vec{\epsilon}}'$ data are of little interest because they contain the effect of the thermopower of the electric field probes,[29] and are not simply related to any microscopic theory. The isothermal thermoelectric tensor $\vec{\vec{\epsilon}}$, as defined by Eqs. (4a), is related to $\vec{\vec{\epsilon}}'$ by the relation $\vec{\vec{\epsilon}} = \vec{\vec{\epsilon}}'\vec{\vec{\gamma}}^{-1}$. The $\vec{\vec{\epsilon}}$ tensor is conceptually more familiar, its component $\epsilon_{11}(0, T) \equiv S$ being the absolute thermoelectric power as involved in the measurement of temperature with a thermocouple. The correction for the Seebeck effect in the leads is simply related to $\vec{\vec{\epsilon}}$ through the relation $\vec{\vec{\epsilon}} = S_{\text{leads}}\hat{1} + \vec{\vec{\epsilon}}'\vec{\vec{\gamma}}^{-1}$. Components of the tensor $\vec{\vec{\epsilon}}$ corrected for the effect of the leads are shown as functions of field at two temperatures in Fig. 3. The thermocouple effect of the leads does not appear in ϵ_{12} but was sufficiently large in ϵ_{11} at the lower fields to render the low-field ϵ_{11} data useless. Both quantities were negative, with ϵ_{11} essentially independent of field and one order of magnitude smaller than ϵ_{12}. Substitution of Eqs. (3) into the Heurlinger relation $\epsilon_{11} = (\epsilon_{11}''\sigma_{11} + \epsilon_{12}''\sigma_{12})/(\sigma_{11}^{2} + \sigma_{12}^{2})$ shows that the high-field value of ϵ_{11} should be independent of field if $\sum_i(\pm)n_i$ is negligible compared to $\sum_i(\pm)n_i H_i^{2}/H^{2}$. This was found to be approximately true in the analysis of σ_{12}, and the thermal effect is characterized by larger H_i values.

A comparison of the data with Eqs. (3) requires that they be put in the form of the kinetic tensor $\vec{\vec{\epsilon}}''$, as defined by Eq. (1). The tensor is related to the corrected $\vec{\vec{\epsilon}}$ tensor by the operation $\vec{\vec{\epsilon}}''$

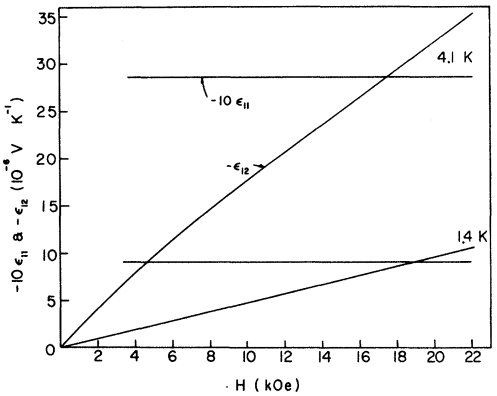

FIG. 3. Isothermal thermoelectric tensor. The coefficient ϵ_{11} is the ordinary thermocouple coefficient, the absolute thermoelectric power, and ϵ_{12} is the isothermal Nernst coefficient. Note that ϵ_{11} is essentially independent of H. Results at the lowest fields were not reliable and are omitted. These are quantities derived from the experimental coefficients $\vec{\vec{\epsilon}}'$ and are corrected for the ϵ of the leads.

$= \overleftrightarrow{\epsilon}\,\overleftrightarrow{\rho}^{-1}$. The inequalities $\rho_{11} \gg \rho_{21}$, $\gamma_{11} \gg \gamma_{21}$, and $\epsilon_{12} \gg \epsilon_{11}$ found in the compensated metal at high field and low temperature allow some simplification. Thus, to first order $\epsilon_{12}'' = \epsilon_{12}/\rho_{11} = -\epsilon_{21}'/\rho_{11}\gamma_{11}$ and $\epsilon_{11}'' = (\epsilon_{11}\rho_{11} - \epsilon_{12}\rho_{21})/\rho_{11}^2$.

The kinetic Nernst coefficient ϵ_{12}'' can, therefore, be computed from the experimental data with reasonable precision, since it involves only a single product of three large measured coefficients and does not involve a correction for the thermocouple effect of the leads. The computation of ϵ_{11}'', however, is very crude. Not only does the computation involve the difference of comparable small quantities, but the term in ϵ_{11}'' involving S_{leads} is roughly 50% of the total effect.[29] Nevertheless, the field and temperature dependence of ϵ_{11}'' computed at six temperatures was found to be self-consistent.

From Eqs. (3c) and (3d) it might be expected that, when $H \gg H_i$, the quantities ϵ_{11}''/T and ϵ_{12}''/T should be independent of temperature. They are not. Their actual behavior is indicated in Fig. 4. Each coefficient has the expected field dependence, ϵ_{11}'' decreasing as $1/H^2$, and ϵ_{12}'' decreasing as $1/H$. Therefore, the excess temperature dependence implies that the density-of-states factors $\sum_i(\pm)Z_i a_i H$ and $\sum_i Z_i$ are temperature dependent. A fit of the high-field results to Eqs. (3c) and (3d) requires that $\sum_i(\pm)Z_i a_i H_i$ and $\sum_i Z_i$ vary from -3.26×10^{37} erg^{-1} cm^{-3} Oe and $+1.95\times10^{34}$ erg^{-1} cm^{-3}, respectively, at 1.4 K to -3.61×10^{37} erg^{-1} cm^{-3} Oe and $+2.31\times10^{34}$ erg^{-1} cm^{-3}, respectively, at 4.1 K.

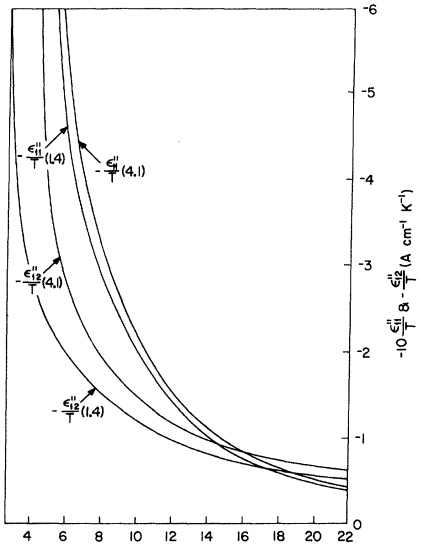

FIG. 4. Kinetic thermoelectric coefficients. The thermoelectric coefficient ϵ_{11}'' and the Nernst coefficient ϵ_{12}'' are shown as functions of field and temperature T. The simplest interpretation of Eqs. (3c) and (3d) leads one to expect that $\overleftrightarrow{\epsilon}''/T$ should be independent of T. The precision of ϵ_{12}'' results is much greater than that of ϵ_{11}'' results.

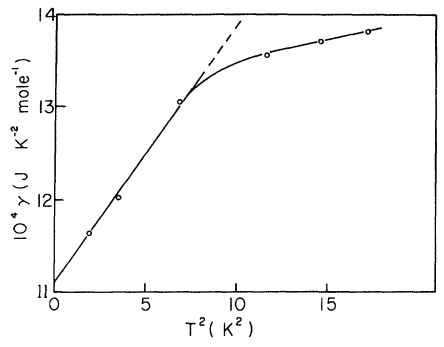

FIG. 5. Nernst specific-heat coefficient. The ϵ_{12}'' data interpreted in terms of Eq. (3d) lead to a prediction of the temperature coefficient γ of the electronic specific heat. The value of γ spans the range of published specific-heat results and displays a monotonic temperature dependence.

The temperature dependence of $\sum_i(\pm)Z_i a_i H_i$ is accountable in terms of the relaxation field H_i which is expected in the thermoelectric effect to display an excess temperature dependence if the ϵ_{11}'' data are to be consistent with the temperature dependence found in the thermal magnetoresistivity γ_{11}, presumably due to vertical scattering processes.

The relaxation field does not appear in the high-field limit of ϵ_{12}''. Like the high-field Hall conductivity σ_{12}, the high-field Nernst coefficient should be independent of the scattering and measure a property of the band structure. The Nernst coefficient is, in principle, an alternative measure of the free-electron density of states as classically determined from the temperature coefficient of the electronic specific heat C_e. The observed temperature dependence of $\sum_i Z_i = 3C_e/\pi^2 k_B^2 T$ is thus not directly explicable in terms of Eqs. (3). This will be discussed further in a following paper. The results for $\sum_i Z_i$ when expressed in terms of a specific heat γ ($C_e = \gamma T$) imply a systematic decrease of γ from 13.8×10^{-4} J mole^{-1}K^{-2} at 4.1 K to 11.7×10^{-4} J mole^{-1}K^{-2} at 1.4 K (Fig. 5). These values are well within the range of values of γ reported from specific-heat measurements on tungsten.[43]

V. CONCLUSION

The high-field magnetotransport effects at liquid-helium temperatures in this rather pure tungsten crystal are, in most respects, amenable to analysis in terms of the asymptotic ($H \gg H_i$) form of a multiband Sondheimer-Wilson theory [Eqs. (3)]. The theory must be empirically modified to allow for a temperature-dependent relaxation time which

is not unique, but different for electrical and thermal processes. Exceptions to this conclusion are the Righi-Leduc coefficients γ_{21} and λ_{12}'' and the Nernst coefficient ϵ_{12}'' which display temperature dependences which are not explicable in terms of the SW equations without still further modifications. This and the appreciable lattice conduction found in the thermal-resistivity data will be considered in a following paper. The relationship between these results and Fermi-surface data must also be considered.

It has recently been noted by Ehrlich[44] that thermal umklapp scattering may be mistaken for electron-electron scattering. This may bear on Eq. (5), the discussion following that equation, and other parts of this work.

ACKNOWLEDGMENTS

The author is indebted to the administration and staff of the Laboratory for Research on the Structure of Matter of the University of Pennsylvania and to Dr. Robert K. MacCrone for their support of, and interest in, the early phases of this work.

*The experiments and preliminary analysis in this work were conducted in the Laboratory for Research on the Structure of Matter of the University of Pennsylvania with support by the Advanced Research Projects Agency of the U. S. Department of Defense under Contract No. SD-69. The work was completed at Virginia Polytechnic Institute with support by the National Aeronautics and Space Administration.

[1]L. Onsager, Phys. Rev. 37, 405 (1931); 38, 2265 (1931).

[2]H. B. Callen, Phys. Rev. 73, 1349 (1948); 85, 16 (1952).

[3]D. Shoenberg, *Low Temperature Physics* LT9 (Plenum, New York, 1965), Pt. B, p. 680.

[4]E. Justi and H. Scheffers, Phys. Z. 37, 700 (1936); 38, 891 (1937).

[5]E. Grüneisen and H. Adenstedt, Ann. Physik 29, 597 (1937).

[6]W. J. de Haas and J. de Nobel, Physica 5, 449 (1938).

[7]J. de Nobel, Physica 15, 532 (1949).

[8]J. de Nobel, Physica 23, 261 (1957); 23, 349 (1957).

[9]W. van Witzenburg and M. J. Laubitz, Can. J. Phys. 46, 1887 (1968).

[10]K. H. Berthel, Phys. Status Solidi 5, 159 (1964); 5, 399 (1964).

[11]N. V. Volkenshteyn, L. S. Starostina, V. Ye. Startsev, and Ye. P. Romanov, Fiz. Metal. i Metalloved. 18, 888 (1964) [Phys. Metals Metallog. 18, 85 (1964)].

[12]E. Fawcett, Phys. Rev. 128, 154 (1962).

[13]E. Fawcett and W. A. Reed, Phys. Rev. 134, A723 (1964).

[14]N. V. Volkenshteyn, V. A. Novoselov, and V. Ye. Startsev, Fiz. Metal. i Metalloved. 22, 175 (1966); 24, 677 (1967)[Phys. Metals Metallog. 22, 15 (1966); 24, 92 (1967)].

[15]R. F. Girvan, A. V. Gold, and R. A. Phillips, J. Phys. Chem. Solids 29, 1485 (1968). The data reported in this largely corroborate and extend an earlier study reported by D. M. Sparlin and J. A. Marcus, Phys. Rev. 144, 484 (1966).

[16]T. L. Loucks, Phys. Rev. 139, A1181 (1965); 143, 506 (1966).

[17]L. F. Mattheiss, Phys. Rev. 139, A1893 (1965).

[18]W. M. Lomer, Proc. Phys. Soc. (London) 80, 489 (1962).

[19]D. E. Soule and J. C. Abele, Phys. Rev. Letters 23, 1287 (1969). This paper reports measurements of the oscillatory magnetomorphic effect in tungsten.

[20]H. J. Trodahl and F. J. Blatt, Phys. Rev. 180, 706 (1969).

[21]J. M. Ziman, *Electrons and Phonons* (Oxford U. P., London, 1960), p. 496.

[22]E. H. Sondheimer and A. H. Wilson, Proc. Roy. Soc. (London) A190, 435 (1947).

[23]A. H. Wilson, *Theory of Metals* (Cambridge U. P., London, 1953), p. 218.

[24]C. G. Grenier, J. M. Reynolds, and N. H. Zebouni, Phys. Rev. 129, 1088 (1963).

[25]C. G. Grenier, J. M. Reynolds, and J. R. Sybert, Phys. Rev. 132, 58 (1963).

[26]See Ref. 21, p. 501 and Ref. 23, p. 320.

[27]T. Heurlinger, Ann. Phys. (Leipzig) 48, 84 (1915); Phys. Z. 17, 221 (1916).

[28]J. R. Long, C. G. Grenier, and J. M. Reynolds, Phys. Rev. 140, A187 (1965).

[29]Data were corrected for magnetoresistance and thermoelectric effects in the cupron wire. The choice of cupron (constantan) wire was unwise. Measurements verified that the W. B. Driver alloy Evanohm is a better choice for such applications. Samples of the constantan-type alloys at 4.2 K showed a negative magnetoresistance varying as $H^{-1/2}$ at low fields and saturating in fields of order 10 kOe to a value about 2% less than the zero-field resistivity. No magnetoresistance was observed in Evanohm. Measurements of the isothermal thermoelectric coefficient of samples from several spools of both alloys against superconducting lead revealed the large value $\epsilon = -0.364T\ \mu\mathrm{VK}^{-1}$ for constantan alloys and the copperlike value $\epsilon = -0.05T\ \mu\mathrm{VK}^{-1}$ for Evanohm. The constantan samples also exhibited some magnetic field dependence of ϵ, but no field dependence of ϵ was exhibited by the Evanohm samples.

[30]L. Colquitt, Jr., J. Appl. Phys. 36, 2454 (1965).

[31]See Ref. 23, p. 310.

[32]See Ref. 21, p. 412; W. G. Baber, Proc. Roy. Soc. (London) A158, 383 (1937).

[33]M. J. Rice, Phys. Rev. Letters 20, 1439 (1968).

[34]E. Fawcett, Advan. Phys. 13, 139 (1964).

[35]See, for instance, E. N. Adams and T. D. Holstein, J. Phys. Chem. Solids 10, 254 (1959).

[36]See, for instance, M. H. Cohen and L. Falicov, Phys. Rev. Letters 7, 231 (1961).

[37]See Ref. 23, pp. 195 and 264.

[38]See Ref. 23, p. 271.

[39]E. Fawcett, Phys. Rev. Letters 7, 370 (1961).

[40]J. Long, Phys. Letters 25A, 677 (1967).

[41]R. S. Blewer, N. H. Zebouni, and C. G. Grenier, Phys. Rev. 174, 700 (1968).

[42]See Ref. 21, p. 386.

[43]See Ref. 16; table on p. 1187 of the first paper.

[44]A. C. Ehrlich, Phys. Rev. B 1, 4537 (1970).